Performance Improvement of LeastSquares Adaptive Filter for High-Speed Train Communication Systems

Irma Zakia* & Adit Kurniawan

School of Electrical Engineering and Informatics
Institut Teknologi Bandung, Jl. Ganesha No. 10, Bandung 40132, Indonesia
*E-mail: irma.zakia@stei.itb.ac.id

Abstract. The downlink communication channel from high-altitude platform (HAP) to high-speed train (HST) in the Ka-band is a slowly time-varying Rician distributed flat fading channel with 10-25 dB Rician *K* factor. In this respect, the received signal is mainly affected by the Doppler shift of the line-of-sight (LOS) link. In order to increase receiver performance, we propose to firstly compensate the Doppler shift of the received signal before least-squares (LS) adaptive filtering is pursued. Implementing the proposed method requires a priori knowledge of the time-varying phase of the LOS component. This is justified since signalling between the train and the controller exists such that the train velocity and location are predictable. Implementing the proposed method to the recursive LS (RLS) received beamforming algorithm shows reduction of mean square error (MSE) and bit error rate (BER).

Keywords: *adaptive beamforming; Doppler shift; high-altitude platform (HAP); high-speed train (HST); least-squares; line-of-sight (LOS); Rician fading.*

1 Introduction

High-speed train (HST) communications exhibit particular phenomena as the train travels with speeds that may reach 575 kmph through its wireless coverage area [1]. The International Telecommunication Union (ITU) specifies the operating frequencies for HSTs served by high-altitude platform (HAP) as 28-31 GHz and 47-48 GHz. Assuming that the train travels in a rural area, the short-term fading channel is time-varying flat fading and Rician distributed. It is modelled as a single ray and a line-of-sight (LOS) component with *K* factor 10-25 dB [2]. Additionally, the physical layer is in accordance with the IEEE 802.16 Single Carrier with bandwidth up to 20 MHz, which yields a slow fading channel [3].

The main problem of the presented channel is the Doppler frequency of the LOS component, where its value depends on the elevation angle between the LOS link and the train velocity vector. Therefore, as long as the train is moving and the elevation angle is not 90°, the receiver suffers from the time-varying phase of the LOS component. In order to decode coherently, the receiver is

Received March 21st, 2016, Revised January 25th, 2017, Accepted for publication April 3rd, 2017.
 ISSN: 2337-5779, DOI: 10.5614/itbj.ict.res.appl.2017.11.2.3

required to track the time-varying channel, or equivalently, follow the direction of the intended signal adaptively.

There are several adaptive filters that can be applied to combat time-varying Rician flat fading channel on high speed train communications. Faletti, *et al.*[2] have implemented the multiple-input multiple-output (MIMO) beamforming recursive least-squares (RLS) algorithm, while examples of single-input multiple-output (SIMO) are given by White, *et al.* in [4] and Zakia, *et al.* In [5], the recursive LS (RLS) MIMO channel estimation algorithm for Rician fading was proposed by Zakia, *et al.* [6] as a generalization to the Rayleigh fading case given in Karami [7]. Both papers present closed-form solutions on the tracking performance in terms of mean square error (MSE). Particularly, Zakia, *et al.* [6] showed that a constant LOS component gives advantage in tracking the channel. This means that the train suffers larger tracking loss as it travels to a lower elevation angle.

Motivated by our previous result presented in Zakia, *et al.* [6], we propose to compensate for the Doppler shift of the received signal before the RLS algorithm is executed. The proposed technique assumes that the time-varying phase of the LOS component is known perfectly at the receiver. This assumption is based on the fact that for high-speed train communications, the speed and train locations can be predicted from communications between trains and the signalling controller center, as shown in Cheng and Fang [8], or by retrieving information from a dedicated environment map, as presented in Li and Zhao [9].

We are aware that our proposed method is similar to that given in Li and Zhao [9]. However, their method is based on a terrestrial system that assumes the channel as frequency-selective so that it employs the weighted average of the Doppler shift of the channel paths, as opposed to a single path Doppler shift compensation as performed here. Moreover, our proposed method is motivated by the analytical work of Zakia, *et al.* [6], which opens up the possibility of extending the result analytically. The performance of the proposed method was analyzed in terms of MSE and bit error rate (BER). Since the proposed method assumes a perfectly known Doppler shift, the BER performance of a more realistic scenario in which imperfection of Doppler shift exists was also evaluated.

We would like to note that the proposed method was first introduced in the author's dissertation, i.e. Zakia, *et al*. [10] but has not been published before. Furthermore, the RLS algorithm implemented here in terms of symbol detection has a different form than that of Zakia, *et al*. [10]. Since the channel considered

is slow fading, we can show that the different forms of symbol detection have negligible impact on system performance.

The method proposed here is applicable to any system that encounters Rician fading with time-varying phase of the LOS component. Firstly, it is not restricted to the RLS algorithm, so it can be implemented to any adaptive filter algorithm, such as least mean squares (LMS) and Kalman. Secondly, even though we assume a single user SIMO beamforming framework similar to the method shown in White, *et al.* [4], Zakia, *et al.* [5], and Rappaport [11], the generalization to the MIMO case is straightforward as long as the Doppler shift of all channel pairs is assumed to be equal. Finally, the purpose of the adaptive filter is not only beamforming, as assumed here, but also channel tracking, like the one used in Zakia, *et al.* [6].

The rest of this paper is organized as follows. Section 2 describes the system model. The proposed method is given in Section 3. In Section 4, the performance of the tracking MSE and BER is evaluated. Finally, Section 5 concludes the paper.

2 System Model

The focus of this paper is the downlink transmission from HAP to train communications with a single $M = 1$ antenna at the HAP and N antennas on the train. The antenna array is mounted on top of the train as an access point (AP) to the passengers inside the train. The communication between the AP and the passengers is not studied here. This results in a SIMO transmission system.

The consideration of implementing a SIMO system is explained as follows. Firstly, although White, *et al.* in [4] investigated a MIMO system that is able to deliver service to single-antenna trains simultaneously, here we assume that only a single train is served by the HAP. Thus, it is not required to have multiple antennas that can provide multiple beams at the HAP. Secondly, the work conducted by White, *et al.* [4] employs an antenna array on the train to partially compensate the high path-loss of the Ka-band frequency and to deal with specular reflections that can occur in urban areas. In this context, the antenna array implemented here is intended to achieve array gain.

The downlink SIMO system presented next, consists of the Doppler model, physical layer standard, fading channel model, and transceiver structure.

2.1 Doppler Model

Since the train is moving with some velocity ϑ (m/s), it induces a Doppler frequency as shown in Eq. (1)

$$F_D = \frac{\vartheta}{c} f_0 \tag{1}$$

where $c = 3x10^8$ m/s and f_0 denote the speed of light and carrier frequency respectively. For the downlink from the HAP to the high-speed train channel, $f_0 = 28$ GHz [3].

As the train moves along its coverage area, the elevation angle between the HAP and the train influence the Doppler shift, K factor, and shadowing [11-13]. The Doppler shift is defined as in Eq. (2):

$$f_D = F_D \cos\psi \tag{2}$$

where ψ denotes the elevation angle. For meaningful communication in the Ka-band, the elevation angle ψ has values in the range $30^\circ \leq \psi \leq 150^\circ$ [4]. Due to the train's velocity, the Doppler shift is elevation-dependent. This yields fast transition of the Doppler shift along one cell coverage, as depicted in Figure 1.

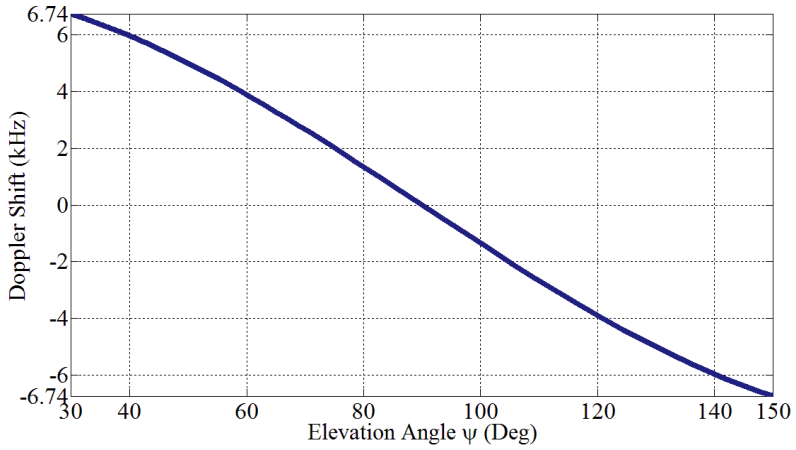

Figure 1 Doppler shift transition.

The HAP is situated at an altitude of 20 km in the stratosphere and is assumed stationary, similar to that assumed in Djuknic, *et al.*[14]. Hence, in this scenario HAP cell coverage is 69.28 km. Assuming the train's speed is 300 kmph, the duration of one cell coverage is thus 13.86 minutes.

2.2 Physical Layer Standard

The HAP channel at the Ka-band shows domination of the LOS component and therefore a single carrier modulation assumption is appropriate [3]. Specifically, the physical layer resembles the IEEE 802.16 for broadband fixed wireless access (FWA) with supported frequency carrier 10-66 GHz and Nyquist root raised cosine (RRC) pulse shaping with 25% roll-off factor. Since the bandwidth is 2-20 MHz bandwidth, the sampling rate is $T_s = 50 - 500$ ns, which in this paper, is assumed equal to the symbol rate.

There are three types of modulation supported by this standard, which can support bit rates up to 120 Mbps. Without loss of generality, it is assumed that QPSK modulation is employed, which results in a 4-40 Mbps bit rate.

2.3 Fading Channel Model

An evaluation of a short-term SIMO fading channel for HAP in high-speed train communication where the channel is time-varying and Rician distributed with K factor 10-25 dB, has been presented in [2]. Although the channel is dominated by the LOS in the Ka-band, the existence of scaterrers due to particles in the atmosphere and trees in the vicinity of the train still yields a non-LOS (NLOS) component. Additionally, assuming the major part of the train tracks are located in a rural area, the channel is considered flat. By employing the aforementioned physical layer standard, the fading is thus slow fading.

The discrete time baseband SIMO channel at time index n is given as in Eq. (3):

$$\boldsymbol{h}[n] = \sqrt{\frac{K}{K+1}}\boldsymbol{h}_{\mathrm{LOS}}[n] + \sqrt{\frac{1}{K+1}}\boldsymbol{h}_{\mathrm{NLOS}}[n] \tag{3}$$

where $\boldsymbol{h}_{\mathrm{LOS}} \in \mathbb{C}^{N,1}$ and $\boldsymbol{h}_{\mathrm{NLOS}} \in \mathbb{C}^{N,1}$ denote the LOS and NLOS channel vectors respectively. Defining $\boldsymbol{a}(\theta_0) \in \mathbb{C}^{N,1}$ as the receiver antenna steering response at a nominal direction of arrival (DOA) θ_0, the LOS channel vector is determined as in Eq. (4):

$$\boldsymbol{h}_{LOS}[n] = \boldsymbol{a}(\theta_0)e^{j2\pi F_D T_s \cos(\psi)n} \tag{4}$$

The statistics of the NLOS channel component is modelled in the time-spatial domain. Assuming independency between the time and spatial domains, the second-order statistics becomes the following Eq.(5) [2]:

$$\boldsymbol{R}[m] = R_{\mathrm{TD}}[m]\boldsymbol{R}_{\mathrm{SD}} \in \mathbb{C}^{N,N} \tag{5}$$

where $R_{\mathrm{TD}}[m] \in \mathbb{C}^{1,1}$and $\boldsymbol{R}_{\mathrm{SD}} \in \mathbb{C}^{N,N}$ yield the second-order time domain autocorrelation at time difference m and the spatial domain autocorrelation matrix respectively.

The time domain autocorrelation assumes Clark's model for Rayleigh fading as defined in Eq. (6):

$$R_{\mathrm{TD}}[m] = J_0(2\pi F_D T_s m) \tag{6}$$

where J_0 is the modified zero order Bessel function of the first kind.

The spatial domain autocorrelation matrix is influenced by the local micro scatterers in the atmosphere, where each micro scatterer introduces a wave arriving at DOA θ. The overall effect of these scatterers is further modelled in Falletti, *et al.* [2] as expressed in Eq. (7):

$$\boldsymbol{R}_{SD} = \int \boldsymbol{a}_{RX}(\theta)\boldsymbol{a}_{RX}^{H}(\theta)p(\theta)d\theta \tag{7}$$

where $p(\theta)$ denotes the probability distribution function (PDF) of the DOA resulting from the micro scatterers. Since the distance of the HAP to the train is much larger than the radius of the micro scaterrers in the atmosphere, $p(\theta)$ is modeled by a Gaussian distribution as determined in Eq. (8):

$$p(\theta) = \frac{1}{\sqrt{2\pi\sigma_\theta^2}} e^{\frac{-(\theta-\theta_0)^2}{2\sigma_\theta^2}} \tag{8}$$

The symbol σ_θ^2 denotes the variance of the DOA θ around its nominal value θ_0. A higher variance value means a less spatially correlated channel.

Besides determination of the channel's second-order statisitics, the value of the K factor is also required. Iskandar, *et al.* have shown that at 1.2 GHz and 2.4 GHz, the K factor is influenced by the elevation angle [12]. There exists no literature that models the K factor in the Ka-band. Despite this, a heuristic approach can be used to adapt the result shown in Iskandar and Shimamoto [12] to the Ka-band characteristic by considering the fact that in the Ka-band, the K factor is 10-25 dB [2]. The relation between the K factor and the elevation angle is shown in Table 1, where for simulation purposes the elevation angles are well represented by 30°, 60°, and 90°.

Table 1 *K* Factor in Ka-band.

Elevation angle	*K* factor
30°	10 dB
60°	18 dB
90°	25 dB

2.4 Transceiver Structure

The SIMO baseband transceiver structure is depicted in Figure 2. The transmission is done on a per frame basis. At the HAP, a number of *P* training symbols followed by a number of *D* data symbols are formed into a frame. The transmitted symbol is defined as $x[n]$, which is either a training or data symbol, depending on the position of time index n at each frame. Without loss of generality, no channel coding is employed at the transmitter.

The symbol $x[n]$ is then passed to the fading channel $\boldsymbol{h}[n]$. After considering the impairment due to additive white Gaussian noise (AWGN) $\boldsymbol{v}[n]$, the received signal becomes the following equation:

$$\boldsymbol{y}[n] = x[n]\boldsymbol{h}[n] + \boldsymbol{v}[n] \in \mathbb{C}^{N,1} \tag{9}$$

where $\boldsymbol{v}[n] \in \mathbb{C}^{N,1}$ is i.i.d. zero mean Gaussian process with variance σ_v^2.

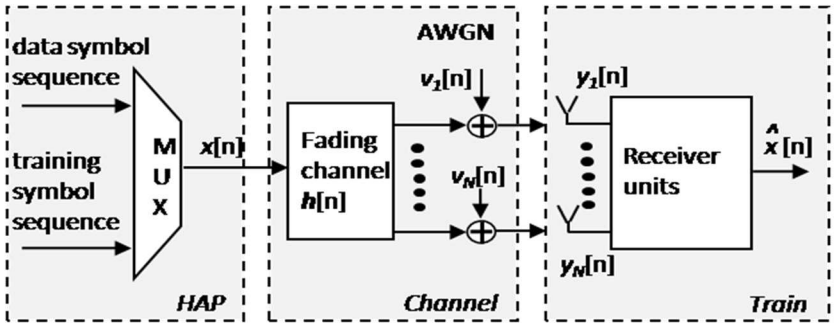

Figure 2 Transceiver structure.

The task of the receiver on the train is to track the channel and use the channel estimates for coherent detection of the transmitted data symbols. For implementation purposes, the RLS algorithm is employed as shown in [15]. On each frame, the *P* training sequence is used to obtain the channel estimates iteratively until a sufficienty low MSE is achieved. This mode is called data-aided (DA) mode. Afterwards, decision-directed (DD) mode is executed, where at each time instant the detected data symbols are used to update the channel estimates iteratively.

3 Proposed Method

Zakia, *et al.* have shown that for a moving receiver, the Doppler shift of the LOS channel component ($\psi \neq 90^{\circ}$) yields worse MSE tracking performance at the receiver [6]. Specifically, the MSE tracking gain achieved when the mobile travels from 0° to 60° is insignificant if compared to when it travels to a 90°

elevation angle. Therefore, we propose to compensate for the Doppler shift of the LOS component before executing the RLS SIMO algorithm. The focus is on the LOS component since for high-speed train communications based on the HAP system in the Ka-band, the channel is predominantely LOS [2].

It is assumed that the variables contributing to the Doppler shift of the LOS component, $F_D \cos\psi$, act as a priori information. This requires to have knowledge of the following variables at the receiver:

1. Train speed – the train speed ϑ determines the Doppler frequency F_D.
2. Train location – the elevation angle information is extracted from the train's location.

For high-speed train communications, the train speed and location information can be obtained for HST due to its repetitive movement characteristic [8-9]. In particular, this information can be obtained from the signalling controller center, as shown in Cheng, *et al.* [8], and can be predicted by retrieving the information from a dedicated radio environment map, as presented in Li, *et al.* [9]. The assumption of Doppler shift of the LOS component known perfectly at the receiver is therefore realistic. Ideas for how these parameters can be tracked in realtime are not considered in this paper; interested readers are referred to Chen, *et al.* [16] and Kay, *et al.* [17] for further details.

Figure 3 illustrates the block diagram of the proposed method. It can be seen that modification is performed with respect to the received signal vector $\boldsymbol{y}$. Mathematically, the modified received signal is determined as in Eq. (10):

$$\tilde{\boldsymbol{y}}[n] = \boldsymbol{y}[n] e^{-j2\pi F_D \cos(\psi) n} \in \mathbb{C}^{N,1} \tag{10}$$

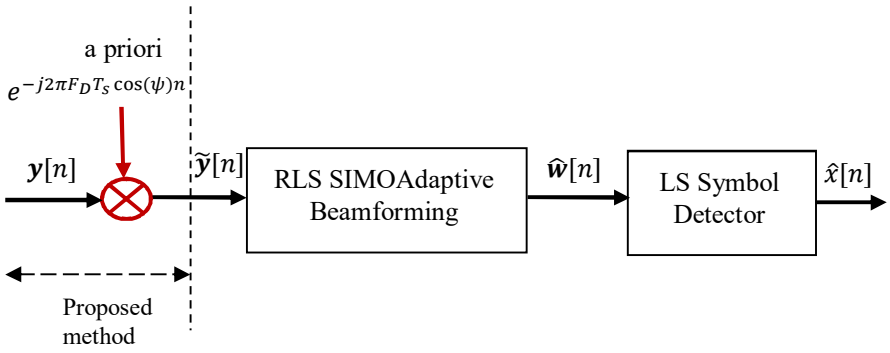

Figure 3 Block diagram of the proposed method [10].

The proposed method is independent of the underlying channel compensation algorithm. Thus, extension to other adaptive filters such as LMS beamforming

presented in [15] or RLS channel estimation presented in Zakia, *et al.* [6] and Karami [7] is straightforward.

The beamforming vector $\boldsymbol{w} \in \mathbb{C}^{N,1}$ in the LS SIMO context minimizes the weighted LS error at time n as shown in Eq. (11):

$$\sum_{i=1}^{n} \gamma^{n-i} |x[i] - \boldsymbol{w}^H[n]\tilde{\boldsymbol{y}}[i]|^2 \tag{11}$$

where γ is the forgetting factor and takes values $0 < \gamma \leq 1$. A higher γ means a higher dependency on the previous error signals, which increases computation. An optimum γ is defined as the γ that yields the lowest possible MSE, where the MSE curve versus time index n is monotonically decreasing [7]. Since no closed-form solution in determining the optimum γ exists for LS beamforming, trial and error was performed in the system simulation.

The estimated beamforming vector $\hat{\boldsymbol{w}} \in \mathbb{C}^{N,1}$ is expressed in Eq. (12):

$$\hat{\boldsymbol{w}}[n] = \left(\sum_{i=1}^{n} \gamma^{n-i} \tilde{\boldsymbol{y}}[i]\tilde{\boldsymbol{y}}^*[i]\right)^{-1} \left(\sum_{i=1}^{n} \gamma^{n-i} \tilde{\boldsymbol{y}}[i]x^*[i]\right) \tag{12}$$

For the purpose of implementation, the calculation of $\hat{\boldsymbol{w}}[n]$ is performed using the RLS algorithm [15] as follows:

Initialization	$\hat{\boldsymbol{w}}(0) = \boldsymbol{0}, \boldsymbol{P}(0) = \delta^{-1}\boldsymbol{I}$
For $n = 1, 2, 3, \ldots$end	do:
Modified received signal	$\tilde{\boldsymbol{y}}[n] = \boldsymbol{y}[n]e^{-j2\pi F_D T_s \cos(\psi)n}$
Temporary value	$\boldsymbol{q}[n] = \boldsymbol{P}[n-1]\tilde{\boldsymbol{y}}[n]$
Gain	$\boldsymbol{k}[n] = \frac{1}{\gamma + \tilde{\boldsymbol{y}}^H[n]\boldsymbol{q}[n]}\boldsymbol{q}[n]$
A priori error	$e[n] = x[n] - \hat{\boldsymbol{w}}^H[n-1]\tilde{\boldsymbol{y}}[n]$
Beamforming vector update	$\hat{\boldsymbol{w}}[n] = \hat{\boldsymbol{w}}[n-1] + e^*[n]\boldsymbol{k}[n]$
Inverse autocovariance update	$\boldsymbol{P}[n] = \frac{1}{\gamma}(\boldsymbol{P}[n-1] - \boldsymbol{k}[n]\boldsymbol{q}^H[n])$

The block diagram of the RLS SIMO beamforming algorithm with modified received signal is visualized in Figure 4, where the bold line shows the signal

vector. The symbol is detected coherently at the receiver. The symbol detection is only required in DD mode. This is because in DA mode, the data symbols are known at the receiver, thus $\hat{x}[n] = x[n]$. In this paper, it is assumed that symbol detection follows the LS approach. Within the RLS algorithm, the symbol detection is written as in the following Eq. (13):

$$\hat{x}[n] = \mathcal{D}(\widehat{\boldsymbol{w}}^H[n-1]\tilde{\boldsymbol{y}}[n]) \tag{13}$$

where $\mathcal{D}(.)$ denotes hard detection.

We would like to emphasize that the symbol detection Eq. (13) has a different form than the one defined in Zakia, *et al.* [10]. Although not shown here, we can verify that due to the slow fading channel assumption, no discrepancy results in the system performance.

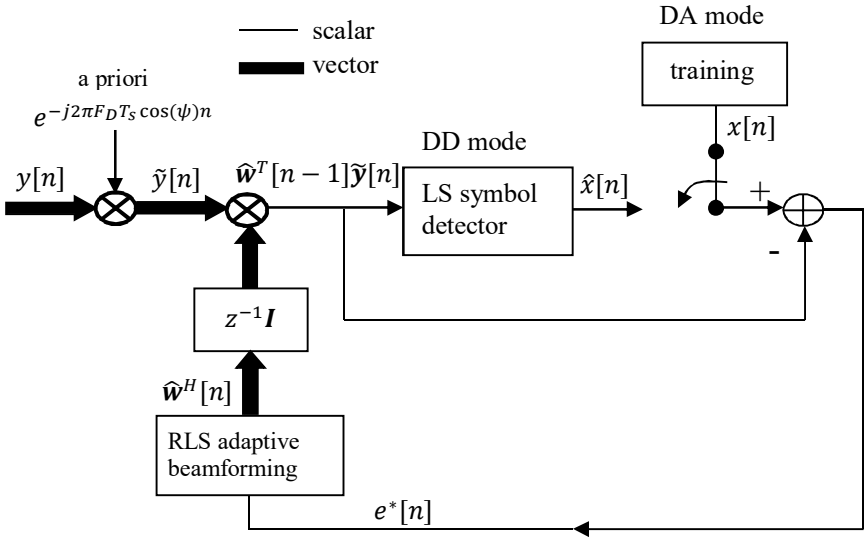

Figure 4 Block diagram of RLS SIMO beamforming.

4 System Simulation

Since the beamforming weight vector is calculated iteratively, the algorithm requires time until it converges. This convergence performance is established from the learning curve, as shown in Haykin [15] and given in Eq. (14):

$$\sigma_e^2[n] = E\{|e[n]|^2\} \tag{14}$$

The learning curve is identical to the a priori error MSE. The rate of convergence depends on γ. Therefore, deciding which γ value is used is crucial in order to achieve convergence and an acceptable and low $\sigma_e^2[n]$.

The performances of the proposed method in terms of MSE and BER were evaluated through Monte Carlo simulations. In determining the MSE, the RLS algorithm was executed in DA mode, whereas for the BER calculation, the algorithm was executed in both DA and DD mode. Specifically, DA mode was carried out until the MSE was low enough. Afterwards, the algorithm was switched to DD mode.

The simulation was performed on two different values of angle spread, i.e.$\sigma_\theta^2 = 0.01$ and $\sigma_\theta^2 = 5$. The former reflects a highly spatially correlated channel, whereas the latter is considered i.i.d. fading. Details on the resulting channel autocorrelation matrix can be found in Zakia, *et al.* [18].

Since no Doppler shift is introduced on the 90° elevation angle, simulation of the proposed method is unnecessary on the $\{K,\ \psi\} = \{25\ \text{dB}, 90^\circ\}$ scenario. Thus, only the $\{K,\ \psi\} = \{10\ \text{dB}, 30^\circ\}$ and $\{K,\ \psi\} = \{18\ \text{dB}, 60^\circ\}$ scenarios were considered. Other parameters used in the simulation are $M = 1, N = 5$, $F_D T_s = 0.00039$.

4.1 Mean Square Error

A simulation was conducted to estimate the beamforming vector $\widehat{\boldsymbol{w}}[n]$ by the RLS algorithm. It was then used to calculate the MSE $\sigma_e^2[n]$ by averaging more than 5000 independent channel realizations. A number of $P = 500$ training symbols was taken. The channel scenario was $\{K,\ \psi\} = \{10\ \text{dB}, 30^\circ\}$. Without loss of generality, the convergence performance was represented by SNR = 6 dB and 10 dB with forgetting factors $\gamma = 0.96$ and 0.99 respectively. The chosen pair of SNR and forgetting factor is only for presentation clarity.

The MSE of the RLS beamforming with compensated received signal for angle spread $\sigma_\theta^2 = 0.01$ and $\sigma_\theta^2 = 5$ are presented in Figures 5 and 6 respectively. It is obvious that the proposed method indeed gives lower MSE, the amount of which depends on the system parameters, which in this case are angle spread, SNR, and forgetting factor. Particularly, by compensating the Doppler shift of the received signal, the time variation of channels dominated by the LOS component (e.g. *K*=10 dB, 20 dB) was considerably decreased. This increases the reliability of old snapshots. Thus, lower tracking MSE for both cases of angle spread $\sigma_\theta^2 = 0.01$ and $\sigma_\theta^2 = 5$ are obtained.

Another interesting observation, depicted in Figures 5 and 6, is that $\gamma = 0.99$ seems too high for RLS SIMO (without compensation) when SNR = 10 dB, $\sigma_\theta^2 = 5$. When γ was set higher than the required optimum value for a certain channel condition, the algorithm was too slow in forgetting the old error signals,

which still yielded a high MSE when converged. After the proposed method was implemented, a higher correlation between the old and the present error signals was noticable due to reduced channel fluctuations. Therefore, with the modified approach, $\gamma = 0.99$ is a good choice, resulting in a sufficiently low MSE.

4.2 Bit Error Rate Performance

Before evaluating the BER performance, the values of γ for each SNR $\in \mathcal{S}$, $\mathcal{S} = \{0,2,4,6,8,10\}$ dB are required. One frame was assumed to have $P = 100$ training symbols and $D = 400$ data symbols. By trial and error, the γ found for each SNR $\in \mathcal{S}$ were $\{0.98, 0.97, 0.96, 0.96, 0.96, 0.97\}$ for angle spread $\sigma_\theta^2 = 0.01$ and $\{0.98, 0.97, 0.97, 0.96, 0.96, 0.99\}$ for angle spread $\sigma_\theta^2 = 5$. The BER was averaged over 15,000 independent channel realizations, which resulted in approximately 10^6 data bits.

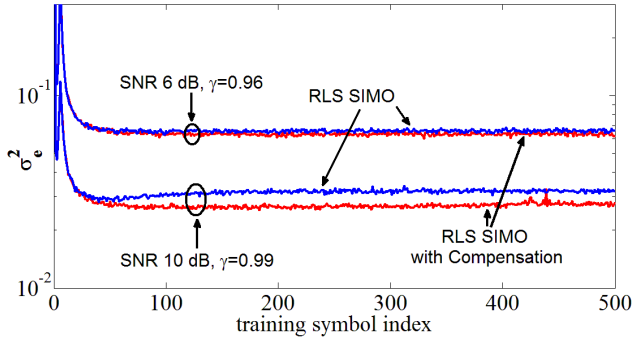

Figure 5 Learning curve for $\sigma_\theta^2 = 0.01$, $\{K, \psi\} = \{10\text{ dB}, 30^\circ\}, P = 500, F_D T_s = 0.00039$.

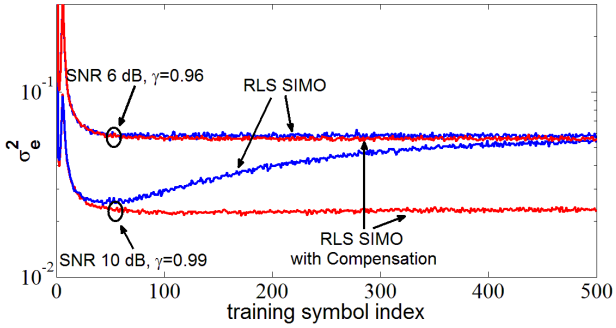

Figure 6 Learning curve for $\sigma_\theta^2 = 5$, $\{K, \psi\} = \{10\text{ dB}, 30^\circ\}, P = 500, F_D T_s = 0.00039$.

Figure 7 visualizes the BER peformance. The baseline reference is the BER for the AWGN channel, which reflects the best possible BER. The BER performance of the RLS algorithm for both angle spreads shows a significant BER gradient decrease as the SNR reaches 10 dB. This is because the estimated beamforming vector $\hat{\boldsymbol{w}}[n]$ is not accurate enough to track the channel variation due to Doppler shift, rendering the detector unable to decide correctly in consecutive detection stages. This phenomenon is called error propagation, which causes the so-called error floor common in systems switching between DA and DD modes [19]. The number of symbols during each mode determines a trade-off between capacity and error floor. In fact, we can show that by sacrificing 25% of capacity, BER performance is reduced to more than one order of magnitude at angle spread $\sigma_\theta^2 = 5$ and SNR 10 dB.

It is also justified in Figure 7 that in the simulated SNR values, the BER and possibility of error floor are both reduced by implementing the proposed method. This means that the proposed method renders the RLS algorithm more robust to channel variation without sacrificing capacity. Moreover, for angle spread $\sigma_\theta^2 = 5$, the BER is decreased by almost two orders of magnitude at SNR 10 dB. This significant decrease shows the robustness of the proposed method to Doppler shift as well as benefiting from fading diversity.

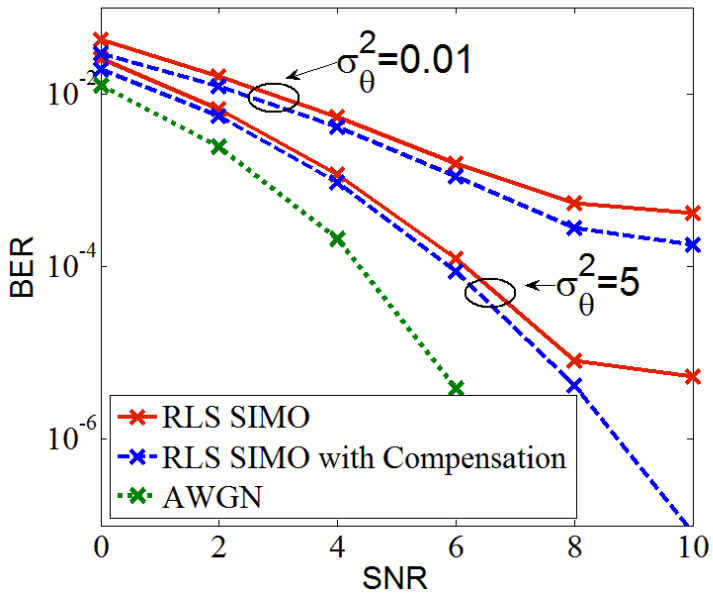

Figure 7 Bit error rate, $\{K, \psi\} = \{10\text{ dB}, 30^\circ\}, M = 1, N = 5, P = 100, P + D = 500, F_D T_s = 0.00039$.

4.3 Bit Error Rate with Imperfect Doppler Information

The proposed algorithm assumes a priori knowledge of train location and speed, such that the Doppler information in terms of $e^{j2\pi F_D T_s \cos(\psi)n}$ is perfectly known at the receiver. This information is further used for compensating the Doppler shift of the received signal. Although railway signalling facilitates information on train location and speed, imperfect channel state information is possible, for example due to delay intransmission and/or processing from the signalling controller unit (at the driver side) to the signal processing unit at an access point (possibly inside the train roof).

For simulating the BER with imperfect channel information, the parameters assumed were $K = 10$dB, $\psi = 30^{\circ}$, $v = 300$ km/jam, $F_D T_s = 0.00039$.

Imperfections of train location lead to erroneous elevation angle ψ. It is assumed that the distance errors are ±11 m and ±500 m, where the first is a common value in the Global Positioning System (GPS) and the latter is to emphasize a worse scenario. The errors in speed are assumed as ±2% and ±5%.

The channel parameters assuming perfect and imperfect apriori knowledge are listed in Table 2. Imperfect apriori knowledge is represented by parameter $F_D T_s \cos\psi$. This knowledge is further used as complex exponential $e^{-j2\pi F_D T_s \cos\psi\, n}$ in order to compensate the received signal.

Table 2 Perfect and imperfect channel parameters.

A priori Knowledge	ψ	ϑ	$F_D T_s \cos\psi$
Perfect	30^0	300 kmph	0.00034
Imperfect: location ±11 m, speed ϑ ±2%	29.99º-30.008º	294-306 kmph	0.00033-0.0003436
Imperfect : location ±500 m, speed ϑ ±5%	29.66º-30.36º	285-315 kmph	0.0003211-0.00036

Depicted in Figure 8 is the BER curve with imperfect apriori knowledge. It is identified that even for high location errors of 500 m and speed errors of 5%, the BER increment is insignificant for the proposed method. The primary reason in this case is because channel parameter$F_D T_s \cos\psi$ is only altered by 6%. A higher $F_D T_s$ is likely to impact a higher loss in BER. It is reasonable to

say that the accuracy of location and speed requirement depends also on system symbol duration T_S.

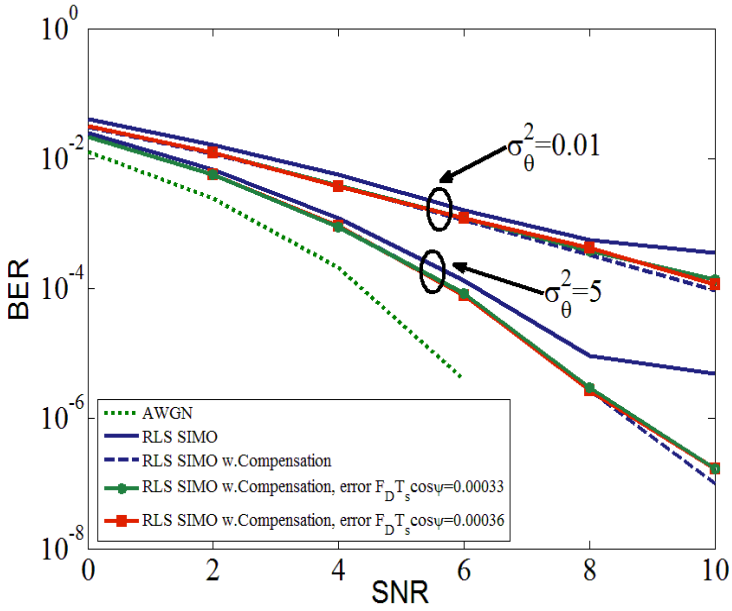

Figure 8 Bit error rate with imperfect a priori knowledge, $\{K, \psi\} = \{10\ \text{dB}, 30^\circ\}, M = 1, N = 5, P = 100,\ P + D = 500,\ F_D T_S = 0.00039$

5 Conclusion

The performance of the RLS received beamforming with Doppler shift compensation in Rician fading channel was given in terms of MSE and BER. By compensating the Doppler shift of the received signal, the time variation of channels dominated by the LOS component was considerably decreased, which from the MSE calculation perspective translates to a higher correlation between the old and present error signals. Thus, for the same forgetting factor the proposed method yields a reduction of the tracking MSE. Additionally, lower BER values by almost two orders of magnitude were found by implementing the Doppler compensation method. This also shows that the proposed method renders the RLS algorithm more robust to channel variation, without sacrificing capacity. For systems working with high symbol rates, insignificant BER losses result due to imperfect a priori knowledge. Attractive issues for future work are analytical determination of the optimum forgetting factor and implementation of the proposed method by using a predicted or estimated Doppler shift.

References

[1] Ai, B., Cheng, X., Krner, T., Zhong, Z., Guan, K., He, R., Xiong, L., Matolak, D.W., Michelson, D.G. & Briso-Rodriguez, C., *Challenges Toward Wireless Communications for High Speed Railway*, IEEE Transactions on Intelligent Transportation Systems, **15**(5), pp. 2143-2158, 2014.

[2] Falletti, E., Sellone, F., Spillard, C. & Grace, D., *A Transmit and Receive Multi-Antenna Channel Model and Simulator for Communications from High Altitude Platforms*, International Journal of Wireless Information Networks, **13**(1), pp. 59-75, 2006.

[3] Mohorcic, M., Javornik, T., Lavric, A., Jelovcan, I., Falletti, E., Mondin, M., Boch, A., Feletti, L., Presti, L., Merino, D., Borio, D., Penin, J., Arino, F. & Bertran, E., *Selection of Broadband Communication Standard for High-Speed Mobile Scenario*, Capanina, http://www.capanina.org/documents/CAP-D09-WP21-JSI-PUB-01.pdf, (10 January 2017).

[4] White, G., Falletti, E., Xu, Z., Borio, D., Sellone, F., Zakharov, Y., Presti, L. & Daneshgaran, F., *Adaptive Beamforming Algorithms for Advanced Antenna Types for Aerial Platform and Ground Terminals*, Capanina, http://www.capanina.org/documents/CAP-D17-WP33-UOY-PUB-01.pdf, 10 January 2017.

[5] Zakia, I., Tjondronegoro, S., Iskandar & Kurniawan, A., *Performance Comparison of LMS and RLS Adaptive Array on High Speed Train Delivered from High Altitude Platforms*, in Proceedings of 2013 International Conference of Information and Communication Technology (ICoICT), pp. 28-32, 2013.

[6] Zakia, I., Tjondronegoro, S., Iskandar & Kurniawan, A., *On the Tracking Performance of Least Squares MIMO Channel Estimation in Rician Fading*, IEICE Communications Express, **3**(1), pp. 27-32, 2014.

[7] Karami, E., *Tracking Performance of Least Squares MIMO Channel Estimation Algorithm*, IEEE Transactions on Communications, **55**(11), pp. 2201-2208, 2007.

[8] Cheng, M. & Fang, X., *Location Information-assisted Opportunistic Beamforming in LTE System for High-speed Railway*, EURASIP Journal on Wireless Communications and Networking, **2012**(1), pp. 1-7, 2012.

[9] Li, J. & Zhao, Y. *Radio Environment Map-based Cognitive Doppler Spread Compensation Algorithms for High-speed Rail Broadband Mobile Communications*, EURASIP Journal on Wireless Communications and Networking, **2012**(1), pp. 1-18, 2012.

[10] Zakia, I., Tjondronegoro, S., Iskandar & Kurniawan, A., *Performance Improvement of Receiver for HAP-Based Communication with High Mobility using Recursive-Algorithm,* PhD Dissertation, School of

Electrical Engineering and Informatics, Institut Teknologi Bandung, Bandung, 2014.

[11] Rappaport, T.S., *Wireless Communications: Principles & Practice*, 1st ed., Prentice-Hall:Upper Saddle River, NJ, 1996

[12] Iskandar & Shimamoto, S., *Channel Characterization and Performance Evaluation of Mobile Communication Employing Stratospheric Platforms*, IEICE Transactions on Communications, **E89-B**(3), pp. 937-944, 2006.

[13] Holis, J. & Pechac, P., *Elevation Dependent Shadowing Model for Mobile Communications via High Altitude Platforms in Built-up Areas*, IEEE Transactions on Antennas and Propagation, **56**(4), pp. 1078-1084, 2008.

[14] Djuknic, G., Freidenfelds, J. & Okunev, Y., *Establishing Wireless Communications Services via High-altitude Aeronautical Platforms: A concept whose time has come?*, IEEE Communications Magazine, **35**(9), pp. 128-135, 1997.

[15] Haykin, S., *Adaptive Filter Theory*, 3rd ed., Prentice-Hall:Upper Saddle River, NJ, 1996.

[16] Chen, P. & Li, H., *An Iterative Algorithm for Doppler Spread Estimation in LOS Environments*, IEEE Transactions on Wireless Communications, **5**(6), pp. 1223-1228, 2006.

[17] Kay, S., *A Fast and Accurate Single Frequency Estimator*, IEEE Transactions on Acoustics, Speech, and Signal Processing, **37**(12), pp. 1987-1990, 1989.

[18] Zakia, I., Tjondronegoro, S., Iskandar & Kurniawan, A., *Received LS Beamforming on Ka-band Channel Model of HAP System*, International Journal on Electrical Engineering and Informatics (IJEEI), **5**(4), pp. 454-473, 2013.

[19] Meyr, H., Moeneclaey, M. & Fechtel, S., *Digital Communication Receivers: Synchronization, Channel Estimation and Signal Processing*, John Wiley & Sons: New York, NY, 1998.